Dynamical evolution of quasicircular binary black hole data

Miguel Alcubierre,[1] Bernd Brügmann,[2] Peter Diener,[3,9] F. Siddhartha Guzmán,[4] Ian Hawke,[5,6] Scott Hawley,[7] Frank Herrmann,[5] Michael Koppitz,[8] Denis Pollney,[5] Edward Seidel,[3,5,9] and Jonathan Thornburg[5]

[1]*Instituto de Ciencias Nucleares, Universidad Nacional Autónoma de México, A.P. 70-543, México D.F. 04510, México*
[2]*Theoretical Physics Institute, University of Jena, 07743 Jena, Germany*
[3]*Center for Computation and Technology, 302 Johnston Hall, Louisiana State University, Baton Rouge, Louisiana 70803, USA*
[4]*Instituto de Física y Matemáticas, Universidad Michoacana de San Nicolás de Hidalgo, Edificio C-3, Cd. Universitaria. C. P. 58040 Morelia Michoacán, México.*
[5]*Max-Planck-Institut für Gravitationsphysik, Albert-Einstein-Institut, Am Mühlenberg 1, 14476 Golm, Germany*
[6]*School of Mathematics, University of Southampton, Southampton SO17 1BJ, United Kingdom*
[7]*Center for Relativity, University of Texas at Austin, Austin, Texas 78712, USA*
[8]*Laboratory for High Energy Astrophysics, NASA Goddard Space Flight Center, 8800 Greenbelt Rd., Greenbelt, Maryland 20771, USA*
[9]*Department of Physics and Astronomy, Louisiana State University, Baton Rouge, Louisiana 70803, USA*

(Received 1 December 2004; published 5 August 2005)

We study the fully nonlinear dynamical evolution of binary black hole data, whose orbital parameters are specified via the effective potential method for determining quasicircular orbits. The cases studied range from the Cook-Baumgarte innermost stable circular orbit (ISCO) to significantly beyond that separation. In all cases we find the black holes to coalesce (as determined by the appearance of a common apparent horizon) in less than half an orbital period. The results of the numerical simulations indicate that the initial holes are not actually in quasicircular orbits, but that they are in fact nearly plunging together. The dynamics of the final horizon are studied to determine physical parameters of the final black hole, such as its spin, mass, and oscillation frequency, revealing information about the inspiral process. We show that considerable resolution is required to extract accurate physical information from the final black hole formed in the merger process, and that the quasinormal modes of the final hole are strongly excited in the merger process. For the ISCO case, by comparing physical measurements of the final black hole formed to the initial data, we estimate that less than 3% of the total energy is radiated in the merger process.

DOI: 10.1103/PhysRevD.72.044004 PACS numbers: 04.25.Dm, 04.30.Db, 04.70.Bw, 95.30.Sf

I. INTRODUCTION

One of the most pressing problems in gravitational physics is the solution of the two body problem for an inspiralling pair of black holes (BHs) from quasicircular orbit to merger. This process is expected to be a likely candidate for early detection by the current generation of gravitational wave detectors. Although considerable success has been made in long term, 3D evolutions of single distorted holes or head-on collisions [1,2], and hybrid numerical-perturbative evolutions [3,4], long-term evolutions of binary BH systems with angular momentum have seen only limited successes [5–8], up to timescales of a single orbit [9]. With limited evolution times, emphasis has been on starting from solutions to the constraint equations which approximate the very last phase of the inspiral process, close to the final plunge.

Such a family of BH binary parameters was proposed by Cook [10], and is based on finding minima of an effective potential for boosted binary BHs (with throats). The effective potential approach was also applied later in [11] for binaries constructed from puncture data, where similar results were found for the innermost stable circular orbit, or "ISCO". Furthermore, recent work [12,13] finds a very similar sequence of orbital parameters for binary puncture BHs using an entirely different construction based on the assumption of a "helical Killing vector" (HKV). On the other hand, Refs. [14–16], the first to develop the HKV approach, solve the thin sandwich equations for binary BHs (with throats), obtaining markedly different results for the estimate of the ISCO. These results agree with increasingly higher order post-Newtonian calculations [17]. At somewhat larger separations, the various constructions show better agreement, as would be expected.

It is critical to understand the differences between these data sets, in particular to investigate whether any of them represent late stages of physically realistic orbital BH mergers. The only method to study the fully nonlinear orbital dynamics of these data sets, which are well into the strong-field region, is full numerical simulation. Recent advances, including the use of the BSSN evolution system [18–21], new gauge conditions [1], and excision techniques [22,23], have brought about significant improvements in the ability of numerical relativity to handle binary systems. Further, by using corotating coordinates (implemented through an adjustment to the shift condition [24]) we find that the BHs can effectively be held in place, greatly reducing dynamics in grid functions and removing complications due to the need of moving excision regions. These improvements have allowed us to carry out the first

systematic and fully nonlinear numerical studies of the orbital dynamics of such data sets, constructed to be in the ''near-ISCO-regime''. The dynamics of the entire inspiral and merger process can be followed to well over $t \approx 100M$ in many cases. (Distances and times are given in terms of the Arnowitt-Deser-Misner (ADM) mass, which is approximately unity for the initial data models studied here.) Similar techniques were recently used to evolve a pair of separated apparent horizons for the expected period of a close orbit [9].

In this paper we apply these full nonlinear capabilities to examine the orbital dynamics of a near-ISCO sequence. The sequence, based on the effective potential work of Refs. [10,11], is constructed to represent a family of circular orbits of nonrotating, equal mass puncture BHs. These parameters were previously studied [4,25] with a hybrid numerical-perturbative approach (see, e.g., [3,26,27]). Increasingly sophisticated over the years, this hybrid approach is aimed at extracting waveforms if a linear regime can be reached, while only fully relativistic approaches are capable of studying the dynamics of the complete inspiral process. The near-ISCO regime studied here is for initial proper spatial separations ranging from $4.99M$ (the Cook-Baumgarte ISCO) to $7.84M$. The data are evolved at least until a common horizon forms, indicating that the pair has merged. In all cases we find that the merger occurs in roughly half (or less) of the expected period, based on the determination of the angular velocity in the initial data calculation. These and other measures discussed below indicate that rather than orbiting BHs, these data sets represent nearly plunging BHs.

Using techniques originally developed in [28–33] and applied to grazing BH collisions in [5,7,8,34], we study the physical properties, such as mass and spin, and the dynamics of the final BH horizons formed in the merger process. In particular, we compare a number of independent measures of horizon dynamics, including the geometry of apparent horizons and event horizons, and the isolated horizon formalism [35–37], which show consistent results for masses and spins of the final black holes. Comparing these results with the parameters of the initial data, we are able to infer some properties of the orbital dynamics. We find that at low resolution, the angular momentum of the final BH is significantly lower than the angular momentum of the spacetime. However, for the case studied in most detail at higher resolution, the angular momentum of the final BH formed in the merger is within about 20% of the angular momentum of the spacetime. Hence, with current resolutions, we are not yet able to use this to measure the angular momentum radiated. On the other hand, our highest resolution calculations of the final BH mass indicate that less than 3% of $M_{\rm ADM}$ is radiated, showing very good accuracy of the overall energy accounting in the simulations, but the current resolutions are still not sufficient to use this measure to predict precisely the radiated energy. By studying the dynamics of the horizon geometry, we are further able to determine the oscillation frequency of the final BH, showing that its quasinormal modes (QNMs) are strongly excited in the merger process.

II. INITIAL DATA

The initial data are calculated via the puncture method [38]. This variant of Brill-Lindquist initial data performs a conformal compactification at the interior asymptotically flat region of the BHs. The extrinsic curvature is given by the Bowen-York solution to the momentum constraint, and the Hamiltonian constraint is solved for the conformal factor. The data are conformally flat and maximally sliced. The initial lapse is chosen to be $\alpha = 1$, while the initial shift is determined by a quasirigid rotation (see below).

Each member of the initial data sequence we consider has two BHs of equal mass and equal opposite momentum, without spin. Initial parameters for such systems in quasicircular orbit are tabulated in [25], based on the effective potential calculations of [10,11] for punctures. In Table I we list the first five elements in this sequence. The effective potential construction singles out QC-0 as representing the presumed innermost stable circular orbit, or ISCO, while other members of the sequence of quasicircular orbits have initial radii progressively further out. We evolve all members of this near-ISCO regime to coalescence and beyond, using full numerical relativity. The measure L/M between the holes is the proper distance computed along a coordinate line from the location of one apparent horizon (AH) to the other. For convenience, we also provide dynamically determined coalescence times in the Table, as measured by the appearance of the horizons, both as computed by coordinate time and by the proper time measured by an observer at the origin between the two BHs. Further discussion of the evolution results are the subject of the following sections, but one can see immediately that by

TABLE I. Elements of the initial data sequence of [25], listing the initial proper separations, angular momenta, and angular velocity (L/M, J/M, $M\Omega$, and corresponding orbital timescale $T_{\rm orbit}$). The coordinate time $t_{\rm AH}$ and the central-observer proper time $\tau_{\rm AH}^{\rm cent}$ to common apparent-horizon formation are given for the intermediate resolution $dx = 0.06M$ runs with shift parameters $(\eta, p, n) = (4, 1, 4)$, corresponding to Figs. 2 and 3. Also shown is the proper time $\tau_{\rm EH}^{\rm cent}$ until a common event horizon is found for a central observer. Due to computational limitations, we did not attempt to locate EHs for QC-2 - QC-4.

Model	L/M	J/M^2	$M\Omega$	$T_{\rm orbit}$	$t_{\rm AH}$	$\tau_{\rm AH}^{\rm cent}$	$\tau_{\rm EH}^{\rm cent}$
QC-0	4.99	0.779	0.168	37.4	16.8	6.71	4.91
QC-1	5.49	0.781	0.142	44.2	19.2	8.49	6.66
QC-2	5.86	0.784	0.127	49.5	21.1	9.76	–
QC-3	6.67	0.794	0.102	61.6	25.4	12.9	–
QC-4	7.84	0.817	0.076	82.7	31.7	17.3	–

these measures, coalescence occurs well before the orbital time scale for all cases studied.

III. EVOLUTION METHODS

Formulation and gauge.—The evolution of the system is carried out using the techniques and evolution system ("BSSN") given in [18–20] with the implementation described explicitly in [1]. We use a hyperbolic version of the "1 + log" lapse and Γ-driver shifts. In particular, the lapse α is evolved using

$$\partial_t \alpha = -2\alpha K, \tag{3.1}$$

where K is the trace of the extrinsic curvature. The shift is implemented using

$$\partial_t \beta^i = F B^i \qquad \partial_t B^i = \partial_t \tilde{\Gamma}^i - \eta B^i \tag{3.2}$$

with η a constant dissipative parameter and F a function of space and time given by

$$F = \frac{3}{4}\frac{\alpha^p}{\psi_{\rm BL}^n}, \tag{3.3}$$

where $\psi_{\rm BL}$ is the time independent conformal factor for Brill-Lindquist data. This choice of F ensures a shift which is nearly static at late times, as well as ensuring the correct falloff near the puncture. The factor $3/4$ guarantees that the asymptotic gauge speed associated with the longitudinal shift components is equal to the speed of light. These features were found to be important for long-term stable and accurate evolutions of head-on collisions without excision [1]. Typically, we use values of $p = 1$ or 2 and $n = 2$ or 4. The parameter η can be used to tune the rate of horizon expansion over the course of the evolution, with larger values leading to faster horizon growth. We typically use values $\eta \in [2, 5]$.

As detailed in [24], we apply a quasirigid rotation to the initial values of the shift vector,

$$\beta^x|_{t=0} = -y\frac{1}{\psi_{\rm BL}}\hat{\Omega} \qquad \beta^y|_{t=0} = x\frac{1}{\psi_{\rm BL}}\hat{\Omega}. \tag{3.4}$$

The factor of $1/\psi_{\rm BL}$ modifying the rigid rotation angular velocity $\hat{\Omega}$ has the effect of ensuring that the shift is zero at the location of the punctures (a condition that is necessary if one wishes that the punctures remain at a fixed location in coordinate space). We find that with appropriate values of $\hat{\Omega}$ in the initial values of the shift, the location of the horizons can be made to remain almost stationary on the grid. Since the size and location of the excision region is determined by the apparent horizon location, this allows the evolution to proceed until merger without requiring the excision region to move on the grid. This type of corotating shift, with dynamic control to adjust the corotating frame as the binaries orbit, is described in [24]. To initialize the corotation $\hat{\Omega}$, experiments were carried out to empirically determine values for which the horizon tended to move least.

It is worth noting that the optimal $\hat{\Omega}$ values tended to be 50%–60% of the values of Ω specified in Table I. As the latter are asymptotically determined, and further as slicing and shift conditions in the interior have strong additional influences on the evolution of the BH orbit (for example, the Γ-driver shift condition used in the evolutions has itself a corotating component [24]), it is difficult to draw firm conclusions from this result. However, the result may be consistent with one of the main results of this paper, namely, that the near-ISCO regime orbital sequences studied here coalesce rapidly, well within an orbital time period, as discussed in more detail below.

Apparent horizons are determined at each time-step using the horizon finder AHFINDERDIRECT described in [39]. As a consistency check, apparent horizons are also determined each $0.48M$ using the earlier, accurate but much less efficient horizon finder AHFINDER, an implementation of the method described in [40,41]. For QC-0 and QC-1, an event-horizon finder [42] was used for further analysis, as a post-processing step.

Numerical methods.— Finite differencing is performed to second order accuracy, and the time stepping is carried out via a 3-step iterative Crank-Nicholson scheme. The boundaries are placed at the same coordinate location for all simulations reported here. The proper distance to the outer boundary is extended by applying a "fisheye" coordinate transformation to the initial data [1,3]. At the outer boundaries, an outgoing-radiation (Sommerfeld) boundary condition is applied to each of the evolution variables. The boundary condition introduces a constraint violation, visible as a region where the constraints do not converge to zero, which propagates inwards from the outer boundary. To minimize the effect of this error on the interior dynamics, we have placed the outer boundaries of our grid at a distance which is causally disconnected (with respect to the physical speed of light) from the common apparent horizon at the time of merger. Although this does not guarantee complete numerical causal disconnection, it significantly reduces potential outer-boundary effects in the neighborhood of the horizons during the premerger phase, and allows us to achieve second order convergence (for instance in the Hamiltonian constraint violation) in the region near the final merged horizon (Fig. 1). Through convergence studies and experiments with boundaries further away, we conclude that with our computational grid parameters, the outer boundary does not affect the results presented here.

Excision.— For the long-term simulations carried out in this paper, we excise the singularity using an extension of the "simple excision" techniques which have proven suc-

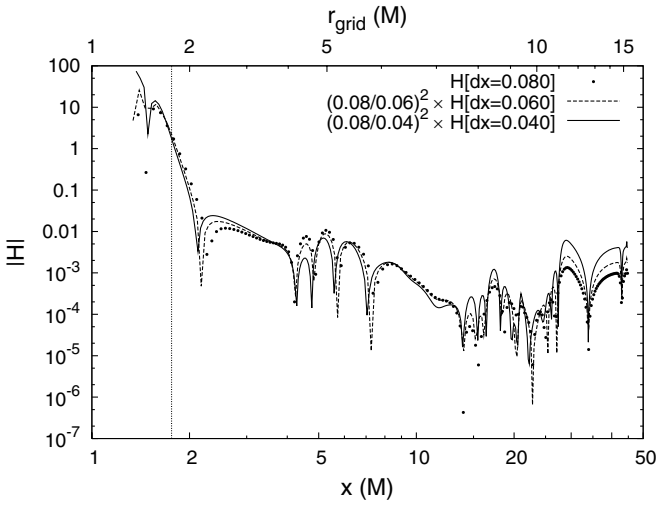

FIG. 1. Convergence in Hamiltonian constraint for the QC-0 case shown at the time of formation of the common AH, $t = 17.76M$. The resolutions are $dx = 0.08M, 0.06M$ and $0.04M$, with the evaluated constraint scaled appropriately so that the lines would lie on top of each other in the case of perfect second order convergence. The lower scale shows the physical distance along the x axis, while the upper scale shows the grid coordinate $r_{\rm grid}$ defined by (4.1). The vertical dotted line shows the apparent-horizon position. Note that although we do not obtain second order convergence near the outer boundary, there is good second order convergence in the neighborhood of the horizons.

cessful in evolving single BH spacetimes [22,23,43]. We use the same condition on each of the fields. Rather than excise a cube we excise within a topologically spherical surface (a ''lego'' sphere) determined by the shape of the AH. A number of buffer points (at least 5) are maintained between the AH and the excision boundary in order to minimize the propagation of errors introduced by the excision boundary condition out of the horizon. As shown in [23], for the gauge conditions used here this buffer zone is expected to be adequate to protect the BH exterior from errors coming from the excision boundary. The excision boundary is allowed to grow as the AH grows, but not to move or shrink in coordinate space—that is, points which are excised are never returned to the active grid. We find that our runs are second order convergent even in areas neighboring this excision boundary. Eventual loss of convergence at late times, after merger, is entirely due to outer-boundary effects.

[1]Note that in our setup, gauge effects can (and do) travel faster than light, so that influences from the boundary can in fact affect the interior evolution at earlier times than the causal separation might suggest. However, empirically we find that constraint violations propagate at the speed of light, as can be seen from, e.g., Fig. 1. Therefore the appearance of the common horizon will not be affected by the boundary.

IV. SIMULATION DOMAIN

For each dataset a number of test runs on a small grid and with low resolution were performed in order to determine the approximate time of common-horizon formation. These times were used to construct grids with outer boundaries causally disconnected from the common horizon at merger time (distance to the outer boundary measured by the physical distance).[1] Initial datasets were set up with punctures along the y-axis and momenta in the x-direction. The z-reflection symmetry allowed the evolutions to be carried out on the positive z portion of the grid, with a symmetry along the $z = 0$ plane implemented through the use of ghost-zones whose data where reflected from interior grid points.

For each model, runs were performed with uniform grid resolutions of $dx = 0.08M$ and $dx = 0.06M$ on grids of $384 \times 384 \times 192$ and $512 \times 512 \times 256$ points, respectively. For 3-level convergence tests, certain models were also run on $640 \times 640 \times 320$ ($dx = 0.048M$) and $768 \times 768 \times 384$ ($dx = 0.040M$), though especially the latter are at the limit of what even large-scale clusters can sustain.

To allow the outer boundary to be farther from the strong-field region, the (Cartesian) grid was placed nonuniformly in the physical coordinates: the physical radius r of each grid point was related to the grid radius $r_{\rm grid}$ by a ''transition fisheye transformation'' ([1])

$$r = a r_{\rm grid} + (1-a)\frac{s}{2\tanh(r_0/s)} \times \left[\ln\left(\cosh\frac{r_{\rm grid}+r_0}{s}\right) - \ln\left(\cosh\frac{r_{\rm grid}-r_0}{s}\right)\right] \quad (4.1)$$

where the parameters $r_0 = 5.5M$ and $s = 0.8M$ are the radius and width of the transition region, and $a = 4$ gives the physical scale factor outside the transition region. This placed the grid boundaries $r_{\rm grid} = 15.48M$ at a physical distance $r = 45.42M$ from the origin.

Figure 1 displays a cross section of the Hamiltonian constraint for QC-0 at $t = 17.76M$ for the three resolutions $dx = 0.08M, 0.06M, 0.04M$, scaled to lie on top of each other if the code is converging at second order. At this time the common horizon has just appeared at the highest resolution. As is typical for these runs for which the outer-boundary condition is not constraint preserving, a nonconvergent effect marches inward from the outer boundary. The region disconnected from the outer boundary, however, shows second order convergence, including points in the immediate neighborhood of the excision region. Significantly, convergence is maintained in the region of common-horizon formation at the time at which it first forms.

V. RESULTS

Evolutions to merger were carried out for each of the QC-0 to QC-4 initial data models, at the 384 and 512 grid

sizes described above (a complete set of 640 and 768 runs was not possible due to computational resource limitations). We study the orbital dynamics and merger times for all five members of this sequence. Evolutions were typically carried out to just beyond the formation of a common apparent horizon (AH), though it is possible with careful parameter choices to carry out the evolutions for significantly longer, often to beyond $t = 100M$. At late times, however, contamination from the outer boundaries can become a significant source of error.

Merger times.— The actual time at which the common AH forms for each model is plotted in Fig. 2 for the resolution $dx = 0.06M$. The coordinate time at which a common AH forms is clearly not a physical invariant, and depends not only on gauge effects, but also on computational parameters. For each point in the near-ISCO QC sequence we have therefore carried out a large number of simulations, varying not only grid resolution and boundary location, but also gauge conditions, within the class of conditions discussed above. We find that the results are only weakly dependent on these effects; based on these tests we have provided approximate error bars in Fig. 2 that span the general range of results we obtained over all parameter variations. Furthermore, we experimented with 4th order spatial and 3rd order temporal differencing, which improves the accuracy of the lower resolution results, but which does not change the essential results presented here. The variations in timing over all gauges and computational parameters tested are typically less than 10%, a result that was typical of earlier studies [7,8,44] where, for example, rather different lapse conditions were also tested with minimal changes in coalescence time results.

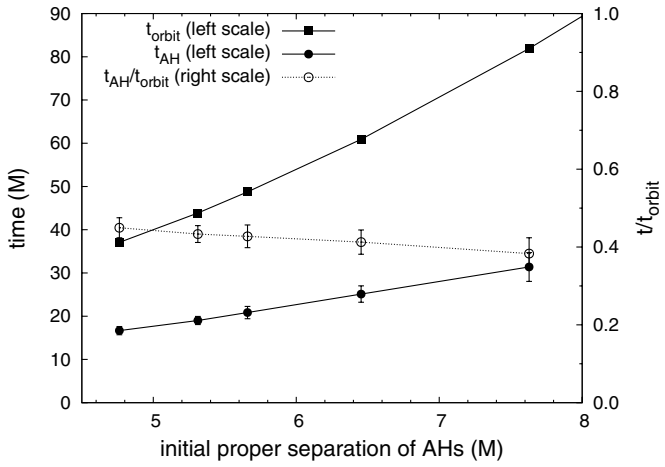

FIG. 2. The time to appearance of a common AH for each of the QC models. Filled circles indicate the results of numerical experiments using $dx = 0.06$, from initial proper spatial separations indicated along the x-axis. The upper line indicates the expected orbital period, based on the initial angular velocity (Table I) and assuming a Newtonian circular orbit. Empty circles indicate the fraction of an orbit before common AH formation. The error bars show $\pm$ the difference between $dx = 0.06$ and $dx = 0.08$ evolutions; the effects of variations in gauge parameters and outer-boundary position are generally smaller than these.

For reference, the expected orbital periods based on the initial data estimate of the angular velocity from Table I are plotted as square points (the topmost curve). For each of the models studied, a common AH appeared in less than half of the expected time for an orbit. This is true even for the further separated cases, well beyond the effective potential ISCO, where dynamics would be expected to better approximate a quasicircular orbit.

To gain insight into the physical interpretation of the merger times, the values obtained from full 3D evolutions of this near-ISCO sequence can be compared to the merger times for head-on collisions, with each puncture starting with zero linear momentum. In Ref. [44] it was shown that there is a remarkable agreement between the Newtonian free-fall time and the fully relativistic computation of the time it takes for a common AH to form for BHs colliding head-on. To do this comparison we carried out a set of 3D simulations, evolving initial data for head-on collisions of BHs represented by punctures initially at the same distances of the QC sequence studied in Table I, but without boosts. We used the same lapse condition as described above for evolving the orbital configurations, while the shift condition was slightly modified.[2] The gauge parameter choices were $p = 1$, $n = 4$ and $\eta \in [2.8, 3.5]$, with the larger values of η being used for the larger separations. We do not expect the small difference in shift condition to affect the results significantly. In Fig. 3, the results of the QC simulations are compared with both Newtonian infall times (dashed line) and relativistic head-on collisions (filled diamonds). The latter two results lie close together on essentially parallel curves, agreeing with the results of [44], and providing a baseline for coalescence times of purely plunging, head-on collisions.

The lower curve in Fig. 3 indicates the proper time to common AH formation, $\tau_{\mathrm{AHcentral}}$, as measured by an observer at the origin of the coordinate system. As this is a symmetry point of the problem, this proper time is invariantly defined and easily calculated by integrating the lapse, and removes most of the potential coordinate ambiguity that might be present in the other time determinations. This proper time $\tau_{\mathrm{AHcentral}}$ is lower than the coordinate time because it is measured in a region where the lapse is somewhat collapsed.

[2]For historical reasons, instead of Eq. (3.2), we have used

$$\partial_t \beta^i = B^i \qquad \partial_t B^i = F \partial_t \tilde{\Gamma}^i - \eta B^i$$

with F, again, given by Eq. (3.3). This has been used in previous studies of head-on collisions [1,23]. We expect that this small difference in gauge will not lead to significant differences in merger times.

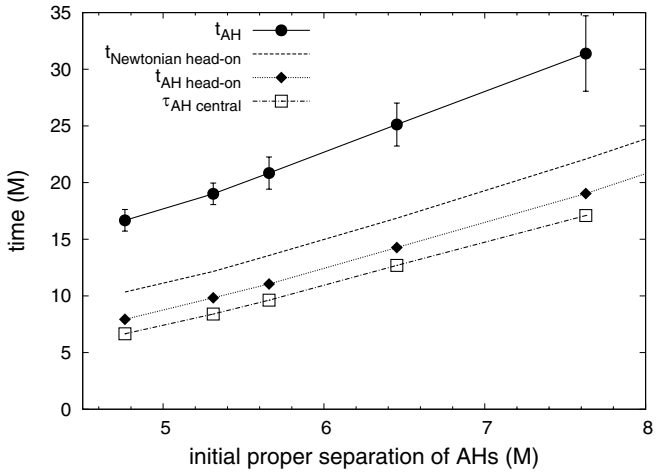

FIG. 3. The time to common AH formation is compared with various head-on collision results. The upper line (filled circles) repeats the curve of Fig. 2, showing common AH formation times for each of the QC models. The dashed line indicates the Newtonian collision time for a pair of particles falling together from the given distance with zero initial velocity. The corresponding relativistic head-on collisions were simulated and give the results plotted as filled diamonds. Finally, the lower curve (open boxes) refers to the same QC simulations as the upper (filled circle) curve, but uses the proper time at the origin at the time of common AH appearance (see text).

It is important to point out that the results obtained for the full near-ISCO QC sequence are basically parallel to the curves for head-on collisions. Further, the proper time measured by observers at the origin, shown by the squares, are also consistent with these results, strengthening the argument that gauge effects are not responsible for the trends. Taken together, these results suggest that for the near-ISCO sequence studied here, the BH's are not in fact in quasicircular orbits, but are rather in an extended plunge towards coalescence. Even at nearly twice the distance of the ISCO (QC-4), there is no clear trend towards an orbit. On the contrary, as shown in Fig. 2, the configurations merge in progressively smaller fractions of an orbit.

Studies of horizon physics.— Much can be learned about the physics of the merger process, and of the final BH formed, through a detailed study of the horizons (see, e.g. [7,8,28,30,32]). We begin by studying the masses of the AHs as a function of time for each member of the sequence. The extent to which horizon masses are consistent with other quantities in the spacetime provides a meaningful and physical measure of the overall accuracy of the simulation. As a measure of the BH mass, we study the irreducible mass $M_{\rm irr} = \sqrt{\rm Area/16\pi}$. In Fig. 4 we plot $M_{\rm irr}$ for each model in the near-ISCO sequence over the course of evolution. Initial individual-horizon masses of approximately $0.5M_{\rm ADM}$ are found to remain essentially constant, until the formation of a common horizon. After merger, we find that in all cases the results are consistent with the

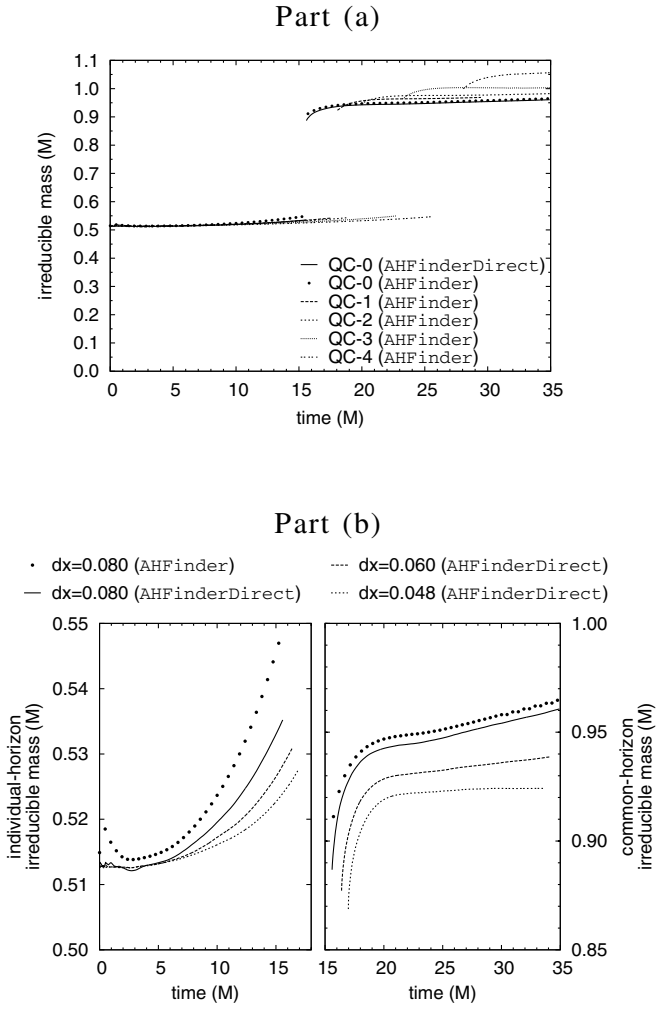

FIG. 4. Evolution of the irreducible mass $M_{\rm irr}$ of the AH as a function of time. Part (a) shows the mass for each QC-N model, for the low resolution $dx = 0.08$ evolutions, showing both individual- and common-horizon masses on the same scale. (For the QC-4 model, the individual AHs are briefly "lost" due to the proximity of the excision region, somewhat before a common horizon is found.) Part (b) shows the mass for the QC-0 model for the $dx = 0.08M$, $0.06M$, and $0.048M$ evolutions, with individual-horizon masses in the left subplot and common-horizon masses in the right subplot. For the $dx = 0.08M$ QC-0 case, results from both apparent-horizon finders are shown, AHFINDERDIRECT as a solid line, AHFINDER as points.

ADM mass, and again hold a rather constant value in the subsequent evolution. Errors in the calculated mass are greater for the late merging cases, but even in the worst cases the masses do not exceed the ADM mass by more than about 5%. Drift in the final horizon mass is quite small, even at late times when errors accumulate and outer boundaries might be expected to have an influence. Results from the two different apparent-horizon finders are very similar, providing a further consistency check.

Figure 4(b) shows that these results are only weakly resolution-dependent. At higher resolutions, we see

slightly smaller horizon masses, somewhat later merger times, and a much smaller upward drift of the common-horizon mass. Unfortunately, these results do not show quantitative convergence. This appears to be due to insufficient resolution, particularly in our coarsest ($dx = 0.08M$) models. (Comparing this result to the good second order convergence of the Hamiltonian constraint at comparable resolutions (Fig. 1), it would appear that the apparent-horizon diagnostics require higher resolution than the Hamiltonian constraint to reach the quantitative-convergence regime.)

Figure 4(b) shows that the individual-horizon masses are slightly greater than $\frac{1}{2}M_{\rm ADM}$. This is not surprising, because we expect a (negative) gravitational binding energy of the two black holes in the initial data, although there is also orbital kinetic energy and possible gravitational radiation in the initial slice not taken into account.

We note that we have not used the traditional measure of mass for a black hole,

$$M_{\rm AH} = \sqrt{M_{\rm irr}^2 + \frac{J^2}{4M_{\rm irr}^2}} \tag{5.1}$$

which includes the angular momentum (and adds a small contribution to the mass), because the angular momentum of the final BH is not known in advance [45,46]. Some previous studies [7,8,30] could safely assume that very little or no angular momentum was radiated, and were therefore able to use angular momentum of the spacetime to compute this mass, and then to calculate the total energy radiated. For the cases studied here, the angular momentum of the final black hole must be measured in each case, as we discuss below.

Beyond simple determination of the AH masses, much more physics of the merger process can be obtained by studying the dynamics of the merged horizons. In this study, in all cases the black holes could be evolved to well past common apparent-horizon formation, allowing numerous physical characteristics of the final black hole to be computed as it settles.

We begin with a study of the shape of the horizons. First, we note that for evolutions that can be carried out to a point of near stationarity, when the final black hole has settled down, the event horizon can be accurately traced by integrating null surfaces backward in time through the spacetime [28,42], and further that a detailed analysis of the physics of these event horizons can be carried out [32,47,48]. We have carried out the analysis for these 3D spacetimes using the method described in [42]. In Fig. 5, we show a comparison of the coordinate locations of the event and apparent horizons for the near-ISCO case QC-1 at various times for a resolution of $dx = 0.08M$. On the initial slice $t = 0$, no common event or apparent horizon exists. Because of the small size of the horizons (compared to the grid spacing), the location of the event horizons can not be found with sufficient accuracy on the initial slice.

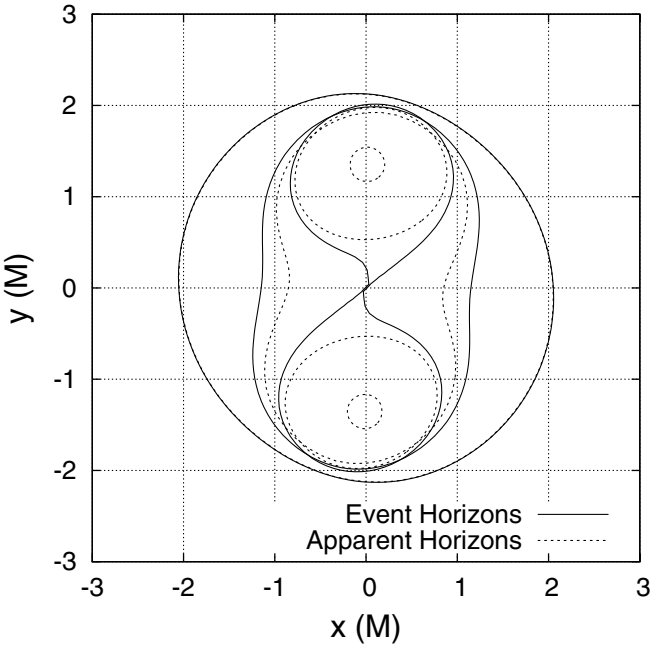

FIG. 5. Event and apparent horizons for an evolution of the QC-1 model ($dx = 0.08M$), showing horizons on the initial slice ($t = 0.0M$), when the EH first merges ($t = 13.0M$), at the appearance of the first common AH ($t = 18.1M$), and at a late time slice ($t = 30.0M$) when the system has essentially settled and the two contours cannot be distinguished anymore.

For that reason we only show the location of the initial apparent horizons. By time $t = 13M$, the event-horizon sections have just merged, with an interesting caustic structure that will be studied elsewhere. Interestingly, away from this caustic region the coordinate locations of the EH and AH agree with great precision, with the EH just outside the AH. By time $t = 18M$, we find the first appearance of a common AH, which as expected occurs later than the merger of the EH. Finally, at the late time $t = 30M$, the AH and EH locations agree very well, indicating the final merged black hole has settled down. The close agreement in location of both local temporal measures (AH) and global temporal measures (EH) of horizon structures gives confidence in the overall accuracy of the merger evolution.

The coordinate location of horizon structures are useful for comparisons and for topology measures, but they say nothing about pure geometric measurements from which physical quantities can be derived. As shown first by Smarr [49] for a Kerr BH, the spin parameter a/m uniquely determines the geometric shape of the BH horizon. As discussed in [28,30], this relation allows one to use the horizon shape as a tool to measure the spin of a black hole in dynamic spacetimes [8,28,30]. A reasonable measure of the shape of BHs that are nearly Kerr is the ratio of proper horizon circumferences measured along polar, C_p, and equatorial, C_e, geodesics [30]. The value of $C_r = C_p/C_e$ is unity for a Schwarzschild BH, and less than unity for

Kerr BHs, with the precise value depending uniquely on the rotation parameter a/m as discussed below. As shown in [30], a distorted rotating BH should oscillate about its equilibrium Kerr shape. In axisymmetry, the polar circumference is uniquely defined, but in full 3D one has multiple choices. In this study, we compute the ratio C_r along circumferii in the coordinate planes (because of symmetry about the plane of the orbit, the equatorial circumference is uniquely defined).

Figure 6 shows results for the case just outside the ISCO, QC-1, plotting the evolution of the ratio of polar to equatorial circumference C_r, measured in the xz plane, for both common apparent and event horizons, for the low resolution case with $dx = 0.08M$. The EH and AH shapes agree extremely well, as was also suggested by Fig. 5. Both curves reveal the oscillation pattern expected in the geometry of a distorted rotating BH formed in the merger.

Following [8,30], we use the oscillation pattern in C_r, and its equilibrium value, to extract important information. The final BH formed during a merger is expected to have its quasinormal modes (QNMs) excited. For each member of the Kerr family, characterized by a/m, a set of discrete QNMs exists. Further, for each (ℓ, m) pair, there is a fundamental mode and higher overtones. In principle, all of these modes may be excited, but in practice the higher overtones are much more strongly damped than the fundamental. Although associated with the potential barrier surrounding the BH, the QNMs excite gravitational waves that propagate both to infinity and also inward, crossing the horizon where they manifest as oscillations in the horizon geometry [28,30]. Therefore, one should find

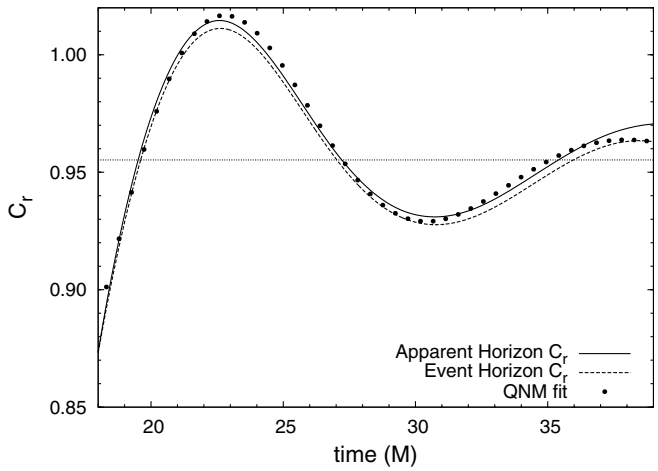

FIG. 6. Comparison of event- to apparent-horizon geometry for case QC-1. The ratio of the polar and equatorial horizon circumferences, $C_r = C_p/C_e$, after formation of common horizons, measured in the xz plane, is shown for the low resolution ($dx = 0.08M$) case. Both the AH and the EH oscillate at the QNM frequency of the final Kerr BH, as confirmed by the fit shown (see text).

various QNMs in the oscillations of C_r, and can use this information to determine the angular momentum of the final BH.

The QNMs for rotating black holes have been studied extensively via perturbation theory, and have been computed as a function of a/m in Refs. [50,51]. Using these known values, and building on previous work [8,30], we have devised the following procedure to analyze the horizon oscillations. One can show analytically that for a Kerr black hole, the quantity C_r has a value given by

$$C_r = \frac{1 + \sqrt{1 - (a/m)^2}}{\pi} E\Big(-\frac{(a/m)^2}{(1 + \sqrt{1 - (a/m)^2})^2}\Big), \tag{5.2}$$

where $E(k)$ is the complete elliptic integral of the second kind

$$E(k) = \int_0^{\pi/2} \sqrt{1 - k\sin^2\theta}\, d\theta.$$

For simplicity C_r can be well approximated by the empirical-theoretical formula, accurate to within less than 1% [30],

$$C_r = \frac{\sqrt{1 - (a/m)^2} + 1.55}{2.55}. \tag{5.3}$$

A perturbed BH horizon with a given value of a/m oscillates about this equilibrium value, largely through a superposition of its QNMs [28,30]. Therefore, the function C_r should be composed of an equilibrium value and a linear combination of various QNMs.[3]. We use an iterative least-squares fitting procedure to determine the value of a/m that best fits the extracted curve C_r.

In these studies, we have found it is sufficient to consider only the offset, and the phase and amplitude of the fundamental modes (given by $\ell - m$) as fitting parameters. Here we have used the $\ell = 2, m = 0, 1, 2$ modes, but we note that unless a/m becomes very large, the QNM frequencies are all very similar to each other. We begin with a fiducial set of modes for a given a/m value, adjust their phase and amplitude and the offset value, which determines the approximate value of a/m through Eq. (5.3) for the first iteration. We then use this value of a/m to choose the QNM frequencies for the next iteration, which through the offset determines the new value of a/m. For the data sets studied here, this procedure converges extremely rapidly, independent of the starting value of a/m. We have also used a binary search technique over a/m to find a minimum error in the least-squares procedure. This method

[3]As shown in [28,30], the horizons oscillate at the tabulated QNM frequencies without need to account for differences in proper time caused by commonly used singularity avoiding slicings, as expected. This can be understood as a canceling of the blueshift of the waves crossing the horizon and the slowing of time by the slicing condition.

gave identical final results for a/m. We note that the fitting procedures use the QNM frequencies for unit BH mass and vary only a/m. This is justified by the fact that $M_{\rm BH} \approx M_{\rm ADM} \approx 1$.

Turning back to Fig. 6 for QC-1, we see that not only do the curves obtained for both the EH and AH closely agree, they both show the oscillations of the final Kerr BH formed in the coalescence process. The result of the fitting procedure to the Kerr modes, described above, is also displayed. We see a beautiful agreement between both the event and apparent-horizon measurements, which are completely independent, and the fit to the QNMs of the final Kerr BH.

This result shows conclusively that in the coalescence process, the QNMs of the final black hole are strongly excited, and dominate the evolution of the horizon after its formation. Although we have not attempted to extract waves in the far zone in these studies, due to the nearness of the outer boundary, this result also implies that at late times QNMs will dominate the waveforms. Below, we study the determination of the spin of the final black hole from this procedure.

In many cases we are able to evolve these systems significantly beyond the formation of the final BH, so that its properties and be studied in depth. We then have additional analysis tools at our disposal. For models where an event horizon was located (QC-0 and QC-1), the horizon generators can in principle provide an independent estimate of the spin of the final black hole, as shown in [28,31,32]. Several factors complicate the analysis of the horizon generators in these cases. First of all, for QC-0 and QC-1, the evolutions did last long enough past merger for us to track the EHs accurately during the merger, but not quite long enough to track them accurately at the time when the black hole has almost settled down to its final stationary configuration. It is only at this late time that the formula relating the generator angular velocity to a/m is correct. Additionally, the angular velocities are gauge dependent. Therefore we have to correct the coordinate angular velocities not only for the effects of our corotating coordinate system but also for any corotation component developed by the Γ-driver shift (Eqs. (3.2) and (3.3)). We have, as yet, not found a satisfactory way of doing this and are consistently getting lower estimates for a/m using the generators compared to the results obtained by fitting QNMs to the EH circumference ratios.

The isolated horizon formalism [52,53] provides an additional tool to study the final horizon to extract physical information. In this case we apply this formalism to the final merged AH to determine a spin by finding an approximate solution to the Killing equation in the surface [35]. While such a solution might not exist immediately after the formation of the common AH we have found that within 7–10M the formalism provides reliable information as shown by the a/m measure approaching a constant value.

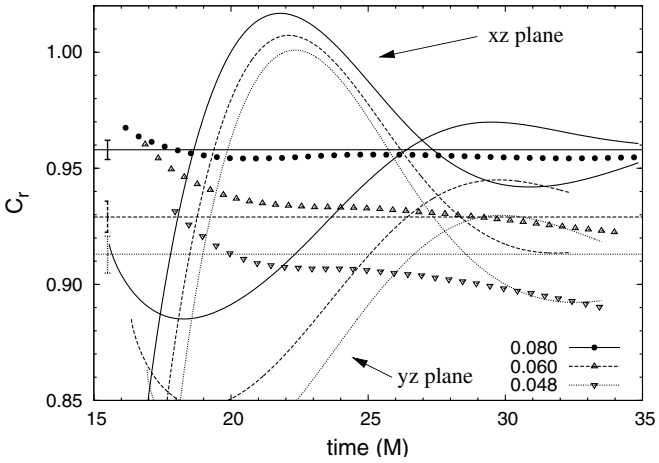

FIG. 7. Comparison of a/m measurements for case QC-0. We show the circumference ratio C_r, measured on the AH, for 3 different resolutions for the two different polar circumferences (computed in the xz and yz plane). We also show the results of the fitting procedure to determine an offset value of C_r (straight lines) for the average of the measurements of circumference ratios as listed in Table II, showing good agreement with the curves. The offsets determined from the two individual fits are used to compute the error bars at the left side of the figure. Also plotted is the result from the isolated horizon computation converted into a circumference measure for comparison. We note that the value from the isolated horizon has developed a plateau between $t = 20 - 25M$, which agrees relatively well with the fits to C_r for the geometric measurements.

We now apply both the horizon geometry and isolated horizon measurements discussed above to the case studied in most depth for this paper, QC-0. First, as noted above, the geometric measurements C_r have been made in two different ways, using the polar circumference in both the xz and yz planes. In Fig. 7 we show the evolution of C_r in both of these planes, as well as a fit to determine the "offset" value, which allows us to estimate the spin of the final BH as described above. For comparison, we have taken the measurement of the isolated horizon spin, and converted it

TABLE II. Table comparing different angular momentum measures a/m for the final black hole in a QC-0 merger simulation at different resolutions dx. C_r refers to a/m determined via a QNM fit as described in the text. The cases xz, yz refer to the ratio of the circumference in the xz to the xy circumference and of the yz to the xy circumferences. The avg denotes the average of the two. IH denotes the value computed by the isolated horizon finder, measured on the plateau at $t = 25M$.

	a/m determined from			
dx	$C_r xz$	$C_r yz$	C_r avg	IH
0.080	0.429	0.471	0.450	0.470
0.060	0.548	0.597	0.573	0.570
0.048	0.603	0.653	0.628	0.660

TABLE III. The table shows the radiated angular momentum and energy for the different resolutions dx for the case QC-0. Starting from Table II we use the minimum and maximum values for a/m at the different resolutions. The ranges given refer to these values for a/m. For the irreducible mass $M_{\rm irr}$ we take the values reported from the apparent-horizon finder at $t = 25M$. We compute the horizon mass $M_{\rm AH}$ which includes angular momentum and then compute radiated energy and angular momentum using initial data values of $M_{\rm ADM} = 1.01$ and $(J/M^2)_{\rm ADM} = 0.779$.

dx	0.080	0.060	0.048
a/m	0.450 ± 0.021	0.572 ± 0.025	0.632 ± 0.028
$M_{\rm irr}$	0.947	0.933	0.923
$M_{\rm AH}$	0.973 ± 0.003	0.978 ± 0.005	0.980 ± 0.006
$J_{\rm rad}$ (%)	45.3 ± 2.9	29.6 ± 3.7	22.1 ± 4.5
$E_{\rm rad}$ (%)	3.61 ± 0.25	3.12 ± 0.45	2.97 ± 0.59

into an instantaneous C_r via Eq. (5.2). We see that this measurement settles into a plateau after about $t = 20M$, agreeing fairly well with the geometric measurements.

In Table II we turn these results into quantitative measurements of the spin of the final BH, for different methods and different resolutions, all for the case QC-0. First, we note that at the lowest resolution, all measurements give consistently low values of the final spin, averaging to $a/m_{\rm lowres} \approx 0.46$. This estimate seems extremely low, however, for a system with initial $J/M^2 = 0.78$. However, the study of resolution effects on this quantity shows that it is very sensitive to resolution. At the highest resolution studied, we measure the final BH to have spin $a/m_{\rm hires} \approx 0.65$. Unfortunately, the various measures used here do not show clear second order convergence properties, and therefore it is not possible to perform a Richardson extrapolation.

Therefore, with present resolution and techniques, we can say with confidence that low resolution simulations underestimate the spin of the final black hole, and that at the highest resolutions possible in the present study, we believe we are still underestimating the final spin by a small amount. A separate investigation of 3D evolution of single, spinning, distorted black holes is underway to investigate resolution and computational parameters needed to accurately resolve and determine the spin from horizon measurements [54]. These results do indicate that the merger process, for the cases studied, radiates a small amount of angular momentum (less than about 20%). The results are summarized in Table III.

Finally, we turn to the computation of the final black hole mass. In Table III we also summarize computations of both the irreducible mass (not including spin) $M_{\rm irr}$ and the horizon mass (including spin) $M_{\rm AH}$ as defined in Eq. (5.1).[4]

[4]We use $J = a/mM_{\rm AH}^2$, and solve the resulting equation for $M_{\rm AH}$.

In computing $M_{\rm AH}$ we use a range of values for a/m, as listed in Table II, to compute the error bars listed in Table III. Note that there are additional errors, in particular, regarding the value of $M_{\rm irr}$ which have not been included. We compute $E_{\rm rad} = (M_{\rm ADM} - M_{\rm AH})/M_{\rm ADM}$ and $J_{\rm rad} = (J_{\rm ADM} - (a/m)M_{\rm AH}^2)/J_{\rm ADM}$. Here we see that, although we are unable to precisely determine the total energy radiated with present techniques, we nonetheless have demonstrated the high degree of accuracy that is now achievable for BH merger simulations. Our highest resolution simulations find a final BH mass within 3% of the ADM mass, and the trend as a function of resolution indicates the total energy radiated to be probably less than this.

We note that Ref. [25] estimated, via completely different methods, that roughly 12% of the angular momentum is radiated, for the same initial data sets studied here, and that the total energy radiated is 3%. These results are consistent with those that can now be obtained via full nonlinear evolution. These points are discussed further below.

VI. DISCUSSION

We have performed the first systematic study of binary black holes constructed to be in approximately quasicircular orbits via effective potential methods, using the full machinery of 3D numerical relativity. The data sets chosen range from the innermost circular orbit, or ISCO (QC-0 in our notation), as determined from this construction, to data sets with separations significantly beyond this, in what we refer to here as the near-ISCO regime. In each case, using a combination of recently developed techniques including excision, new gauges, the BSSN formulation, and a corotating frame, we have been able to carry out the evolutions until after a common apparent horizon formed, indicating an upper bound on the time of merger of the two black holes.

The coordinate times at which the common horizon formed were found to be significantly less than the timescale of an orbit, defining this timescale from the initial angular velocities. We also show that as one evolves initial data sets further out in this near-ISCO-regime, the holes merge after longer times but for progressively smaller fractions of an orbit. We compared these results with results from head-on collisions from corresponding distances, and found that the time to merger shows a very similar trend. This suggests that the initial data models studied here are already in an extended plunge, and not in quasicircular orbits as one might expect from the effective potential considerations. We also found that the angular velocity of the corotating frame needed to keep the holes in a ''head-on'' collision as seen in coordinate space, is roughly $2/3$ of what would be expected from considerations of the initial data, even after one takes into account the intrinsic corotating component of the shift condition used [24]. This result is consistent with our findings that

the holes are merging much more rapidly than expected from initial data considerations.

It is important to point out that these results are also consistent with two completely different studies, the Lazarus results about the near-ISCO-regime, and investigations of binary neutron star systems near the ISCO.

The same black hole data sets that we used here have been studied in the hybrid perturbative-numerical Lazarus approach [3,4,55]. This approach evolves the same data sets numerically, only to a ''linearization'' time, of roughly $10M$, where the two holes are close enough that the system could be treated as a single perturbed BH, after which a perturbative approach was used to complete the evolution. Recall the results from Lazarus on the linearization time along the initial data sequence. According to Ref. [25], for the cases studied here, QC-0 to QC-4, the linearization time increases with separation, but with a slope similar to, or even less than, that seen for coalescence times found here. This result gives support to the notion that this black hole sequence is not approaching an orbital configuration out to QC-4.

Simulations of inspiral sequences of binary neutron stars were carefully studied by Miller and Miller *et al.* in [56,57], who examined the correlation of waveforms from model evolutions against post-Newtonian waveform templates. These authors find strong evidence that the circular orbit assumption can give rather poor approximations for two neutron stars in the near-ISCO-regime. Extrapolating these results to the binary BH case, note that the initial separations of QC-0 to QC-4 clearly fall into the regime where, based on [56,57], one would not expect an orbital configuration. Again, this is consistent with our results that indicate a plunging configuration for all data sets studied here.

A number of issues surrounding the merger time numbers that we have presented need to be considered with care, in particular, effects due to boundary treatment, numerical resolution, and the gauge choice.

We have taken some care to assure that boundary effects do not significantly alter the orbital dynamics and merger times picture. Boundaries have been placed at a distance causally separated from the common horizon, although even without this restriction we have obtained essentially identical runs with boundaries in both closer and further separations, indicating that they do not strongly influence the local dynamics of the black hole horizons for the timescales considered here. Though the numerical domain of dependence is larger, the Hamiltonian constraint was found to converge to second order in the region of the common horizon. We also found that the merger times are not significantly affected by the resolutions used in these studies.

As a point of reference, in Ref. [57], high resolution ($0.054M$) was required to get convergent results. Our coarsest resolution of $0.08M$ is somewhat lower than this, but our medium and high resolutions ($0.06M$ and $0.048M$) are comparable. Unlike [57], we were able to ensure that the outer boundary remains causally disconnected from the merger region for all models studied. As a result, we found that changes to the outer boundary location had only small effects on the time of merger (well within the error bars of Fig. 2).

As remarked above, our studies indicate that for these BH simulations resolution and boundary location effects are not responsible for the quick coalescence times, especially for the cases closer to the ISCO (e.g., QC-0,1).

In addition to resolution and boundary effects, gauge effects will have an influence on the time at which a common AH can first be found. In order to remove some potential slicing and coordinate ambiguity, for all cases we computed the proper time to common AH formation along the origin, which is at all times a point of symmetry between the holes. This measure of time is actually gauge invariant for EHs, but differs from time measured at infinity. The results show the same trend as above, that the holes are in an extended plunge and the greater separations do not show any tendency towards approaching an orbit.

As described above, we have used a consistent set of gauge parameters for all the reported results (except the EH results). Variations of these parameters (to the extent that was possible while still obtaining a long-lasting run) were found to vary the time to appearance of a common AH by only a small amount, within the displayed error bars. However, in the initial $5M$ of evolution when the black holes are still quite small on the grid, resolution effects can influence the rate at which the gauges evolve (collapse of the lapse, for instance), resulting in an offset even with identically chosen gauge parameters. The error bars displayed in Fig. 2 are not statistically derived, but rather show $\pm$ the difference between $dx = 0.06$ and $dx = 0.08$ evolutions; the effects of variations in gauge parameters and outer-boundary position are generally smaller than these. We have not, however, observed a significant increase in the time to common apparent-horizon formation for any of the studied models. In particular for the QC-0 and QC-1 cases where a large number of runs under various conditions of gauge and resolution were carried out, we do not expect the merger time to vary greatly with changes to computational parameters (gauge, resolution, boundary).

On the other hand, as indicated by the growing error bars, there is increasing uncertainty in the QC-3 and QC-4 cases. We note, for example, that the fisheye coordinate transformation that stretches the coordinates in physical space is very close to the initial puncture locations in these cases. This, or additional gauge effects, could conceivably affect orbital evolution properties. Further experiments for initial data in this regime and beyond are underway with mesh refinement, and with a wider range of gauges, and will be reported in future publications.

We also applied a number of tools to measure various physical quantities from the final BH horizons formed in the merger, which were found to agree well. Both event and apparent horizons were determined for the QC-0 and QC-1 cases.[5] Geometric measures of the EH and AH horizon geometry were used to compute the mass and spin of the final BH, as well as the oscillation frequency of the horizon. In all cases, the final BH mass was found to be close (within 4%) to the ADM mass of the spacetime, providing a global measure of the accuracy of the simulations. Appearing with a delay of $4 - 5M$ from the first joining of the EH, the common AH was found to coincide with the EH extremely well very soon after it merged. As we discuss below, in the highest resolution studies of the case QC-0, going beyond overall consistency of energy measures, we are nearly able to predict the total energy radiated.

We also used the isolated horizon formalism to study the dynamics of the final BH, especially the final spin, and obtained similar results. It is interesting that within a few M of common AH formation, the estimate of the final angular momentum of the merged black hole from the AH distortion (via C_r, defined above) and the same measure of EH distortion, agree well with the independent estimate obtained by the isolated horizon formalism. This suggests that it takes only a very short time for the final black hole to settle to a sufficiently Kerr-like state so that each of the approaches can be used. The fact that three very different measures of the spin of the final black hole agree so closely with each other gives us confidence in the validity of the results.

However, the low resolution evolutions consistently under-predict the estimated spin by a significant amount for the cases studied. The resolution studies indicate that at higher resolution, the spin and mass measurements of the final BH horizon approach the asymptotic ADM values, indicating that total radiation is small. For the QC-0 case studied in depth, we estimate that roughly 20% or less of the total angular momentum is lost in the merger process. It is important to note that although the spin of the final black hole is sensitive to the resolution, the coalescence time is not. Even for the more distant configurations in the pre-ISCO family studied here, resolution affects the coalescence time only relatively weakly, and the highest resolution studies find the holes to coalesce well before an orbital time period even for QC-4.

We singled out the ISCO case, QC-0, for very detailed study. In addition to the calculations that indicate the system to radiate of order 20% or less of its angular momentum, we also studied the radiated energy as a function of resolution. By taking into account the estimated angular momentum of the final black hole formed in the merger, we were able to compute the total mass of the final BH, M_{AH}, defined by Eq. (5.1). In all cases, it was found to be within 4% of the ADM mass, and at the highest resolution we found results consistent with 3% or less of total energy being radiated.

Note that the results of the Lazarus approach [4,25] for the total energy and angular momentum radiated are consistent with our fully numerical results for the same initial data. The fact that the results are similar, yet the simulations were carried out with completely different evolution equations (ADM vs. BSSN) and gauge conditions (maximal/zero shift vs. 1+log/Gamma-driver shift), and then were further differentiated by the linear and nonlinear approaches, gives added confidence in the results.

The primary focus of this paper has been on the orbital dynamics of a family of binary black holes expected to be in quasicircular orbits, and not on the waveforms generated. However, by making detailed measurements of the apparent and event-horizon geometries, we have been able to show conclusively that the quasinormal modes of the final black hole are strongly and cleanly excited, and they are dominated by the fundamental $l = 2$ modes. These QNMs will therefore be very strongly seen in the waveforms far from the holes.

While the simulations reported in this paper were being analyzed for publication, another study was carried out using similar techniques, but with a different code [9]. In that study, another binary black hole data set, from a family which is similar to the family studied here but with $L/M = 9$, further beyond the ISCO than the present study (QC-4 has $L/M = 7.84$), was found to evolve beyond the predicted orbital time period ($114M$) without finding a common apparent horizon. Although our results show a trend for this family of data sets to be in near plunge when $L/M < 8$, the results in [9] for $L/M = 9$ are not necessarily in contradiction with the findings of this study. Further, there are a number of differences in the methodology, including gauge conditions and the computational grid setup. In this paper, we have stressed the importance of sufficient resolution to determine accurately the angular momentum of the final black hole. At the same time, we have not seen a strong dependence of the coalescence time on the resolution for the range of simulations carried out here. We note that although our highest resolution runs are for $dx = 0.04M$, slightly coarser than the typical fine grid resolution $dx = 0.03125M$ reported in [9], we would not expect this alone to account for the differences. Detailed study, beyond the scope of the present investigation, will be required for data sets further into the near-ISCO regime to investigate these results.

The question arises at which point of the QC sequence there is a transition from plunge to inspiral. For sufficiently large separations this type of initial data is known to be a good approximation to quasicircular post-Newtonian data

[5]Event horizons for the other cases would have required longer runtimes, or deeper excision regions, necessitating a parameter study of available gauges.

[10,13]. The results presented here indicate that the effective potential method does not produce data sets that will evolve in quasicircular orbits at initial proper separations less than $8M$. We note that for a different initial data set the ISCO was found at an approximate distance of $L/M = 6.61$, much further out than with the method of minimum effective binding energy used for this study [14,15,17].

Recent progress in the use of mesh refinement in our codes [9,58], as well as the introduction of higher order finite difference operators, will enable us to minimize resolution-dependent effects. Work is in progress to investigate the transition in the initial data between orbiting and plunging black holes, and to study the sequence of initial data sets developed using the HKV conformal thin sandwich approach [14,15,17,59].

ACKNOWLEDGMENTS

The authors would like to thank Erik Schnetter and Ryoji Takahashi for many useful conversations and contributions. Results for this paper were obtained using computing time allocations at the AEI, CCT, LRZ, NCSA, NERSC, PSC and RZG. We use Cactus and the CACTUSEINSTEIN infrastructure with a number of locally developed thorns. This work was supported in part by DFG grant ''SFB Transregio 7: Gravitationswellenastronomie'', by NSF Grant Nos. PHY-02-18750, PHY-02-44788 and PHY-03-54842, by the EU Programme 'Improving the Human Research Potential and the Socio-Economic Knowledge Base' (Research Training Network Contract HPRN-CT-2000-00137), by NASA Grant No. NNG04GL37G and by DGAPA-UNAM Grant Nos. IN112401 and IN122002.

[1] M. Alcubierre, B. Brügmann, P. Diener, M. Koppitz, D. Pollney, E. Seidel, and R. Takahashi, Phys. Rev. D **67**, 084023 (2003).
[2] P. Anninos, J. Massó, E. Seidel, and W.-M. Suen, Phys. World **9**, 43 (1996).
[3] J. Baker, B. Brügmann, M. Campanelli, and C. O. Lousto, Classical Quantum Gravity **17**, L149 (2000).
[4] J. Baker, B. Brügmann, M. Campanelli, C. O. Lousto, and R. Takahashi, Phys. Rev. Lett. **87**, 121103 (2001).
[5] B. Brügmann, Int. J. Mod. Phys. D **8**, 85 (1999).
[6] S. Brandt, R. Correll, R. Gómez, M. F. Huq, P. Laguna, L. Lehner, P. Marronetti, R. A. Matzner, D. Neilsen, and J. Pullin *et al.*, Phys. Rev. Lett. **85**, 5496 (2000).
[7] M. Alcubierre, W. Benger, B. Brügmann, G. Lanfermann, L. Nerger, E. Seidel, and R. Takahashi, Phys. Rev. Lett. **87**, 271103 (2001).
[8] E. Seidel, Prog. Theor. Phys. Suppl. **136**, 87 (1999).
[9] B. Brügmann, W. Tichy, and N. Jansen, Phys. Rev. Lett. **92**, 211101 (2004).
[10] G. B. Cook, Phys. Rev. D **50**, 5025 (1994).
[11] T. W. Baumgarte, Phys. Rev. D **62**, 024018 (2000).
[12] W. Tichy, B. Brügmann, and P. Laguna, Phys. Rev. D **68**, 064008 (2003).
[13] W. Tichy and B. Brügmann, Phys. Rev. D **69**, 024006 (2004).
[14] E. Gourgoulhon, P. Grandclément, and S. Bonazzola, Phys. Rev. D **65**, 044020 (2002).
[15] P. Grandclément, E. Gourgoulhon, and S. Bonazzola, Phys. Rev. D **65**, 044021 (2002).
[16] G. B. Cook, Phys. Rev. D **65**, 084003 (2002).
[17] T. Damour, E. Gourgoulhon, and P. Grandclément, Phys. Rev. D **66**, 024007 (2002).
[18] T. Nakamura, K. Oohara, and Y. Kojima, Prog. Theor. Phys. Suppl. **90**, 1 (1987).
[19] M. Shibata and T. Nakamura, Phys. Rev. D **52**, 5428 (1995).
[20] T. W. Baumgarte and S. L. Shapiro, Phys. Rev. D **59**, 024007 (1999).
[21] M. Alcubierre, B. Brügmann, T. Dramlitsch, J. A. Font, P. Papadopoulos, E. Seidel, N. Stergioulas, and R. Takahashi, Phys. Rev. D **62**, 044034 (2000).
[22] M. Alcubierre, B. Brügmann, D. Pollney, E. Seidel, and R. Takahashi, Phys. Rev. D **64**, 061501(R) (2001).
[23] M. Alcubierre, B. Brügmann, P. Diener, F. Herrmann, D. Pollney, E. Seidel, and R. Takahashi, gr-qc/0411137.
[24] M. Alcubierre, P. Diener, F. S. Guzmán, S. Hawley, M. Koppitz, D. Pollney, and E. Seidel, in preparation.
[25] J. Baker, M. Campanelli, C. O. Lousto, and R. Takahashi, Phys. Rev. D **65**, 124012 (2002).
[26] A. Abrahams, D. Bernstein, D. Hobill, E. Seidel, and L. Smarr, Phys. Rev. D **45**, 3544 (1992).
[27] A. M. Abrahams, S. L. Shapiro, and S. A. Teukolsky, Phys. Rev. D **51**, 4295 (1995).
[28] P. Anninos, D. Bernstein, S. Brandt, J. Libson, J. Massó, E. Seidel, L. Smarr, W.-M. Suen, and P. Walker, Phys. Rev. Lett. **74**, 630 (1995).
[29] P. Anninos, D. Bernstein, S. Brandt, D. Hobill, E. Seidel, and L. Smarr, Aust. J. Phys. **48**, 1027 (1995).
[30] S. R. Brandt and E. Seidel, Phys. Rev. D **52**, 870 (1995).
[31] J. Libson, J. Massó, E. Seidel, W.-M. Suen, and P. Walker, Phys. Rev. D **53**, 4335 (1996).
[32] J. Massó, E. Seidel, W.-M. Suen, and P. Walker, Phys. Rev. D **59**, 064015 (1999).
[33] B. Brügmann, Phys. Rev. D **54**, 7361 (1996).
[34] B. Brügmann, Ann. Phys. (Berlin) **9**, 227 (2000).
[35] O. Dreyer, B. Krishnan, D. Shoemaker, and E. Schnetter, Phys. Rev. D **67**, 024018 (2003).
[36] A. Ashtekar, C. Beetle, and S. Fairhurst, Classical Quantum Gravity **16**, L1 (1999).
[37] A. Ashtekar and B. Krishnan, Living Rev. Relativity **7**, 10 (2004).
[38] S. Brandt and B. Brügmann, Phys. Rev. Lett. **78**, 3606 (1997).

[39] J. Thornburg, Classical Quantum Gravity **21**, 743 (2004).
[40] C. Gundlach, Phys. Rev. D **57**, 863 (1998).
[41] M. Alcubierre, S. Brandt, B. Brügmann, C. Gundlach, J. Massó, E. Seidel, and P. Walker, Classical Quantum Gravity **17**, 2159 (2000).
[42] P. Diener, Classical Quantum Gravity **20**, 4901 (2003).
[43] M. Alcubierre and B. Brügmann, Phys. Rev. D **63**, 104006 (2001).
[44] P. Anninos, D. Hobill, E. Seidel, L. Smarr, and W.-M. Suen, Phys. Rev. D **52**, 2044 (1995).
[45] L. L. Smarr, Phys. Rev. Lett. **30**, 71 (1973).
[46] D. Christodoulou, Phys. Rev. Lett. **25**, 1596 (1970).
[47] R. A. Matzner, E. Seidel, S. Shapiro, L. Smarr, W.-M. Suen, S. Teukolsky, and J. Winicour, Science **270**, 941 (1995).
[48] S. A. Caveny, M. Anderson, and R. A. Matzner, Phys. Rev. D **68**, 104009 (2003).
[49] L. L. Smarr, Phys. Rev. D **7**, 289 (1973).
[50] E. W. Leaver, Proc. R. Soc. A **402**, 285 (1986).
[51] E. Seidel and S. Iyer, Phys. Rev. D **41**, 374 (1990).
[52] A. Ashtekar, C. Beetle, and S. Fairhurst, Classical Quantum Gravity **17**, 253 (2000).
[53] A. Ashtekar and B. Krishnan, Phys. Rev. Lett. **89**, 261101 (2002).
[54] P. Diener, R. Takahashi, D. Pollney, and E. Seidel, in preparation.
[55] J. Baker, M. Campanelli, and C. O. Lousto, Phys. Rev. D **65**, 044001 (2002).
[56] M. Miller, Phys. Rev. D **69**, 124013 (2004).
[57] M. Miller, P. Gressman, and W.-M. Suen, Phys. Rev. D **69**, 064026 (2004).
[58] E. Schnetter, S. H. Hawley, and I. Hawke, Classical Quantum Gravity **21**, 1465 (2004).
[59] G. B. Cook and H. P. Pfeiffer, Phys. Rev. D **70**, 104016 (2004).